UCRL- 90437
PREPRINT

CONF-840370--3

RAPIDLY CONVERGENT ALGORITHMS FOR 3-D TANDEM AND STELLARATOR EQUILIBRIA IN THE PARAXIAL APPROXIMATION

UCRL--90437

DE84 009188

Brendan McNamara

This paper was prepared for submittal to
U.S. - Japan Workshop on 3-D MHD Simulation
Oak Ridge National Laboratory
Oak Ridge, TN.
March 19-22, 1984

April-1984

Lawrence Livermore National Laboratory

DISCLAIMER

RAPIDLY CONVERGENT ALGORITHMS FOR 3-D TANDEM AND STELLARATOR EQUILIBRIA IN THE PARAXIAL APPROXIMATION

BRENDAN McNAMARA,

Lawrence Livermore National Laboratory, University of California, Livermore, California.

Tandem and stellarator equilibria at high β have proved hard to compute and the relaxation methods of Bauer et al. [1], Chodura and Schluter[2], Hirshman [3], Strauss [4], and Pearlstein et al. [5] have been slow to converge. This paper reports an extension of the low-β analytic method of Pearlstein, Kaiser, and Newcomb [6] to arbitrary β for tandem mirrors which converges in 10-20 iterations. Extensions of the method to stellarator equilibria are proposed and are very close to the analytic method of Johnson and Greene [7] - the "stellarator expansion". Most of the results of all these calculations can be adequately described by low-β approximations since the MHD stability limits [8] occur at low β. The tandem mirror, having weak curvature and a long central cell, allows finite Larmor radius effects to eliminate most ballooning modes and offers the possibility of really high average β. This is the interest in developing such three-dimensional numerical algorithms.

2. CONNECTION BETWEEN KINETIC AND FLUID MODELS

Tandem mirrors have very large mirror ratios and large flux-surface distortions and so any numerical representation of the equilibrium must use the field lines as the basis of the coordinate system to place mesh points where they are needed. This is done by defining the magnetic field in terms of two scalars (ψ,θ) as

$$\underline{B} = \nabla\psi \times \nabla\theta \qquad (1)$$

which ensures that $\nabla\cdot\underline{B}=0$. In a Stellarator the field lines lie on magnetic surfaces which naturally identify a set of flux surfaces, ψ. In tandem mirrors the field lines are open and there are no natural magnetic surfaces. However, the systems are designed so that confined particles move on closed drift surfaces and, in many designs, these are arranged to be the same surfaces for almost all particles whose orbits intersect the same field line. These are the so-called omnigenous drift surfaces of Hall and McNamara [9] and are physically the relevant choice for ψ. The second flux-line coordinate, θ, is an angle-like variable chosen to satisfy eqn.1. Even in systems which are not everywhere omnigenous for particles moving in the vacuum field alone it is speculated that the plasma transport processes set up radial electric fields which re-align the drift orbits much closer to an omnigenous set and this is to be expected also in toroidal systems. The assumption of omnigenity allows one to connect the microscopic distribution functions with macroscopic density and pressure profiles most easily. Most fusion systems now have neutral beam or high-power RF inputs which directly affect distribution functions and thereby affect the equilibria, effects which need to be modelled.

Tandem mirrors tend to self-anneal for a number of reasons which need further explanation. In stationary electric and magnetic fields the strong constants of motion of a single particle of charge, e, mass, m, and velocity, v are the energy,

$$H = \frac{1}{2} m v_{\cdot}^2 + \mu B + e\Phi \tag{2}$$

and the magnetic moment,

$$\mu = \frac{m v_{\perp}^2}{2B} \tag{2}$$

The magnetic moment is an adiabatic invariant and is destroyed by plasma oscillations at or above the cyclotron frequency, but is not affected by the global geometry of the field, provided the Larmor parameter, ε = (Larmor radius)/(radial scale) is small. The longitudinal adiabatic invariant, Λ, is the action in the bounce motion,

$$\Lambda = \int v_{\parallel} \, dl \tag{3}$$

$$= \int \left(\frac{2}{m}(H - \mu B - e\Phi)\right)^{1/2} ds \tag{4}$$

In the paraxial equilibrium theory [10] it is found that $B=B(\psi,s)$ in a mirror cell at high β. (β= the ratio of plasma to magnetic pressure). The distance s along a field line is approximately the distance, z, along the axis of the system and so $\Lambda = \Lambda(H,\mu,\psi)$ if Φ is small. The drifts are dominated by the ∇B drift and the surfaces are locally omnigenous.

At low β, B is independent of ψ and so the drift surfaces are determined by the difference between s and z due to the weak field line curvature. At this point I introduce Newcomb's [10] notation for the covariant components of the field line curvature,

$$\underline{k} = \hat{b}\cdot\nabla\hat{b}$$

$$= R\nabla\psi + I\nabla\theta \tag{5}$$

Then, it can be shown that the net drift off a surface, ψ, in one bounce of a particle is

$$\Delta\psi = -\left(\frac{m}{e}\right)\int (v_{\parallel}^2 + \mu B) \, I \, \frac{dz}{v_{\parallel}} \tag{6}$$

If B is symmetric about the center of this cell then the integral will vanish if I is designed to be antisymmetric and the drift surfaces will be omnigenous.

In the paraxial limit the potential is determined by the requirement of local quasineutrality and then $\Phi=\Phi(B,\psi)$. Even in a low-β mirror cell which is not omnigenous in the vacuum magnetic field, omnigenity is restored by the potential, determined by radial losses and events in neighbouring cells. An example of just such a case is the GAMMA-VI experiment [11], in which the end plugs are aligned so that fans of field lines enetering the center-cell from the plugs are both vertical. There are NO confined magnetic drift surfaces in the centre cell and so the choice of ψ is determined by the drift surfaces of the high-temperature plasma in the plugs. These are omnigenous locally, with a

circular section at the midplane of each plug. These cicles map into an elliptic cross-section flux tube in the center cell. When the center cell is filled with plasma the radial losses lead to radial potential drops of $\Phi \simeq 3\text{-}4\ T_{ic}$ and the drifts are dominated by the $\underline{E}\times\underline{B}$ drifts and so the total system becomes omnigenous. Reasonable models of the total pressure tensor can be given in the forms

$$\underline{P} = \underline{P}(\Psi,B)$$

$$= \omega(\Psi)(\hat{p}_{\parallel}(\Psi,B)\underline{I} + \underline{bb}\hat{p}_{\perp}(\Psi,B)) \tag{11}$$

where most of the Ψ-dependence has been extracted in the density profile factor ω, and $\underline{P}$ depends only on weakly varying functions like the mirror ratio, or on the radial variation of Φ. The electric fields have not been included in the rest of this paper but will be essential in a fuller model of the tandem mirror equilibria.

3. THE CURRENT BALANCE ALGORITHM.

Newcomb and Strauss have derived the paraxial form of the equilibrium equations from the static and dynamical equations respectively. I therefore present only the most direct definition of the required relations. In addition to the requirement that $\nabla\cdot\underline{B}=0$, which is satisfied by the representation in eqn. (1), the three-dimensional equilibrium of a guiding center plasma is described by the force-balance equation,

$$\underline{J}\times\underline{B} = \nabla\cdot\underline{P} \tag{12}$$

and Ampere's law,

$$\nabla\times\underline{B} = \underline{J} \tag{13}$$

In Strauss' reduction of the dynamical equations, the leading order equilibrium condition, $O(\lambda^0)$, comes from the perpendicular components of the force-balance. Eqns. 12 and 13 can be combined to give

$$\nabla_{\perp}(B^2/2 + p_{\perp}) = \underline{k}(B^2 + p_{\perp} - p_{\parallel}) \tag{14}$$

In the paraxial approximation the curvature is small, $O(\lambda^2)$, and, on dropping the curvature, eqn. 14 may be integrated to give

$$B^2/2 + p_{\perp} = B_v(z)^2/2 \tag{15}$$

This is to be solved for $B(\Psi,z)$ to establish perpendicular pressure balance, where z is the distance along the axis of the system and B_v is the vacuum field on the axis. The next order equilibrium condition is obtained from the parallel component of the force balance, which is

$$\underline{b}\cdot\nabla \cdot \underline{P}=0 \tag{16}$$

This arises from conservation of (H,μ). The pressure gradient is now determined in flux coordinates, along with the perpendicular current flow. It remains to find the parallel current and the actual shape of the flux surfaces. At this point, the Lagrangian representation of the field is introduced in terms of the position of a field line as

$$\underline{X} = \underline{X}(\Psi,\theta,s) \tag{17}$$

so that

$$\underline{B} = \delta B = \underline{X}' B \tag{18}$$

and $\underline{X}'=\partial\underline{X}/\partial s$ is the tangent vector. The parallel current per unit flux, i, is defined as

$$\underline{B} \cdot \underline{J} = iB^2 \tag{19}$$

$$= B\underline{X}'\cdot\nabla\times\underline{X}'B$$

$$= B\underline{X}'\cdot(\nabla B\times\underline{X}' + B\,\nabla\times\underline{X}')$$

$$= B^2\underline{X}'\cdot\nabla\times\underline{X}' \tag{19}$$

In the paraxial approximation only the axial current contributes and so

$$i_1 = i(\Psi,\theta,z) = \frac{\partial X'}{\partial y} - \frac{\partial Y'}{\partial x}$$

$$= B([X',X] + [Y',Y]) \tag{20}$$

where (x,y,z) are Cartesian coordinates and (X,Y,z) the position of a field line. The conversion to (Ψ,θ,z) coordinates introduced the bracket notation for

$$[f,g] = \frac{\partial f\partial g}{\partial\Psi\partial\theta} - \frac{\partial f\partial g}{\partial\theta\partial\Psi} \tag{19}$$

$$= f_\Psi g_\theta - f_\theta g_\Psi \tag{21}$$

and the Jacobian, in this approximation is

$$\frac{I}{B} = [X,Y] \tag{22}$$

The definition of the parallel current involves only local quantities, the position of the field lines, but the equilibrium equations also demand that

$$\nabla\cdot\underline{J} = 0$$

$$= \nabla\cdot\underline{J}_\perp + \underline{B}\cdot\nabla\, i \tag{23}$$

After substituting for $\underline{J}_\perp$ from the force balance eqn. (12), and a little manipulation, i is found to be the field-line integral

$$i(\Psi,\theta,s) = \frac{1}{\sigma}\int_{-L}^{s} \underline{\hat{b}}\cdot\underline{k} \times \nabla(\sigma B^2)\frac{dl}{B^2} + i_{-L} \tag{24}$$

where

$$\sigma = 1 + \left(\frac{p_\perp - p_\parallel}{B^2}\right) \tag{25}$$

The initial plane, s=-L, can be an arbitrary plane in the vacuum outside the tandem mirror where the integration constant, i_{-L}, is zero. In the paraxial approximation,

$$i_p = i(\Psi,\theta,z) = \frac{1}{\sigma}\int_{-L}^{z} 2\hat{+}0\, \frac{\partial \bar{p}}{\partial \Psi}\frac{dl}{B^2} + O(\lambda^3) \tag{26}$$

where

$$\bar{p} = (p_\perp + p_\parallel)/2 \tag{27}$$

The current balance algorithm moves the field lines to equate the local expression, (20), and the integral expression (26)

$$i_l = i_p \tag{28}$$

This is equivalent to setting the integral of the parallel component of the curl of the force balance to zero in Strauss' dynamical model.

The starting position for the tandem-mirror field lines is obtained from one vacuum field line close to the axis of the system of an actual coil configuration. This gives the field strength, $B_v(z)$, and the ellipticity factor, $c_v(z)$ for the field line coordinates

$$X = \rho \cos\theta\, e^{c_v(z)}$$

$$Y = \rho \sin\theta\, e^{c_v(z)} \tag{29}$$

The radial factor, ρ, is chosen to give the correct Jacobian, (13), with $B(\Psi,z)$ calculated from the pressure balance, (18):

$$\rho^2 = \int_0^{\Psi} \frac{d\Psi}{B(\Psi,z)} \tag{30}$$

This choice of ρ takes care of the diamagnetism of the plasma and usually provides most of the displacement of the field lines from their equilibrium positions.

Subsequent movement of the field lines must be done incompressibly so as to preserve the pressure balance,(15), and also the Jacobian, (22), conservation of which is used as numerical test of the accuracy of the calculations. Such a motion is determined by a velocity potential or two-dimensional 'Hamiltonian', u, for the (X,,Y) motion in each z-plane as

$$d\underline{X}(\Psi,\theta,z)/dt = \nabla u \times \hat{z} \tag{31}$$

If the displacement is small then

$$\underline{X} = \underline{X}_0 + \nabla(\int u\, dt) \times \hat{z} + O(\Delta X^2)$$

$$= \underline{X}_0 + \nabla U \times \hat{z} \tag{32}$$

or, in (Ψ,θ,z) coordinates,

$$X = X_0 + B[X_0,U]$$

$$Y = Y_0 + B[Y_0,U] \tag{33}$$

This may be substituted into the current balance eqn.(28), and i_1 linearised to give the equation for U

$$\nabla^2 \frac{(BU)'}{B} = (i_0 - i_p) + [U,i_0] - B[X_0,BU[X_0,\frac{B'}{B}]]$$

$$-B[Y_0,BU[Y_0,\frac{B'}{B}]] + O(U^2) - \frac{1}{2}\bar{i}_p \tag{34}$$

where

$$i_0 = B([X_0',X_0] + [Y_0',Y_0]) \tag{35}$$

Since it does not linearise conveniently, the integral is evaluated, to all orders in U, from the field line positions at the previous step in the iteration process. The right hand side of (34) is evaluated on each plane and the elliptic operator is inverted. The boundary conditions for the tandem mirror are that U=0 on the symmetry planes, $\theta=0,\pi/2$, and at a distant wall, $\Psi=\Psi_{wall}$.

The last piece in (34) is needed to symmetrize the numerical representation of the equation. The tandem mirror has ying-yang symmetry about the mid-point and so computations are done only in an octant of the configuration. By definition, every term of (34) has this symmetry exactly, except for the integral, i_p, which is done from z=-L. Without the symmetrizing addition, which goes separately to zero at equilibrium, the midplane is driven away from equilibrium. Needless to say, some meditation was needed to introduce this correction to ther numerics.

A final integration then yields:

$$U = \frac{1}{B}\int_0^z (BU)' \, dz + \frac{\Phi(\Psi,\theta)}{B(\Psi,z)}$$
$$= U_A + \frac{\Phi}{B} \qquad (36)$$

The integration constant, Φ, on each field line is now determined by the condition that the integral form of the current should vanish in the symmetrically placed vacuum at z=+L.

$$\frac{I_p}{\omega_\Psi} = \frac{i_p(\Psi,\theta,L)}{\omega_\Psi}$$
$$= \oint \frac{dz}{B} \frac{2\bar{p}_\Psi}{\omega_\Psi} \left(X_{0\theta}\, X_0'' + Y_{0\theta} Y_0''\right)$$
$$+ \oint \frac{dz}{B} \frac{2\bar{p}_\Psi}{\omega_\Psi} \left\{ \left(B[X_0,U_A]_\theta\, X_0'' + X_{0\theta}\left(B[X_0,U_A]\right)'' + (X \to Y)\right)\right.$$

$$+ a\Phi_{\theta\theta} + b\Phi_{\Psi\theta} + c\Phi_\Psi + d\Phi_\theta + e\Phi + O(U^2)$$

$$= 0 \qquad (37)$$

The function Φ and its derivatives come out of the integral, yielding a second-order parabolic equation! This is somewhat strange for an equilibrium problem and is a consequence of the paraxial approximation and the conversion of the corresponding axial boundary condition on the dynamical formulation into an integral constraint. It does not occur in the fully three-dimensional treatments (cf. Hall and Mcnamara). The coefficients (a-e) are the corresponding pieces of the integrals over U_A and need not be written explicitly here, except for 'a' which turns out to be the flute stability integral

$$a = \oint \frac{dz}{B} \frac{2\, R\, \bar{p}_\Psi}{\omega_\Psi} \qquad (38)$$

This would vanish at the flute stability boundary, with dire consequences for the algorithm , but this would always be at betas above the stability limit for ballooning or rigid-displacement modes.

The factor $1/(\omega_\Psi)$, is inserted in the integrals to keep all the coefficients finite near the plasma boundary, where the whole equation would otherwise vanish, leaving no useful means of defining Φ. This would also allow the equation to be extended into the vacuum region but Φ will then never satisfy any particular radial boundary condition. There is no current in the vacuum driven by plasma pressure and it seems incorrect to use the constraint on these field lines. This leaves Φ completely unspecified in the vacuum and it can therefore be chosen to be any smooth function which matches to the plasma Φ and which satisfies $\Phi=0$ at $\Psi=\Psi_{wall}$.

The other boundary conditions on Φ are therefore $\Phi=0$ on the symmetry planes $\theta=0,\pi/2$ and, because of the overall quadrupole symmetry of tandem mirrors, at $\theta=\pi/4$, about which Φ is actually anti-symmetric. Only one boundary condition in the Ψ-direction can be specified in the plasma, $\Phi(\Psi=0) = 0$, and this parabolic equation is then integrated outwards from the magnetic axis. This completes the definition of U and the field line displacements needed to achieve equilibrium.

This completes the description of the basic algorithm.

4. APPLICATION TO STELLARATORS.

I have not written a code for the Stellarator version of this method but believe it is a straightforward modification. The first change is to insert an appropriate analytic guess at the initial conditions, similar to eqns (29-30). The next point is to confine the problem volume to one period of the Stellarator and apply periodicity conditions to the calculation. Thus, the integration constant, i_{-L}, in eqn (24) is a given function of Ψ, corresponding to the net induced current flowing on each surface.

The constraint on the parallel current flow is that it be periodic , which yields a pair of conditions on the integration constant Φ and its surface average. Thus, $i_p(\Psi,\theta,L)=i_p(\Psi,\theta,2L)=i_p(\Psi,\theta,nL)$. The second part of this leads to the requirement that the surface average of the parallel current should equal $i_{-L}(\Psi)$. The first part is constructed by iterating the mapping of the field line positions at z=0 to their positions at z=L to get the locations at z=2L. The periodicity requirement then gives an eqn similar to (37).

5. A TMX-UPGRADE EXAMPLE

This particular example was the first case successfully brought to equilibrium by L.D.Pearlstein with the dynamical code in some 11,000 time steps. The result shown is very close to that and both are close to the TEBASCO result from the low-β analytic theory.

The first figure shows the axial magnetic field profile as $B_{kG}(Z_{cm})$.

Improved accuracy is obtained by stretching the z coordinate and Fig2 shows B(s(z)). The initial analytic guess at equilibrium gives the parallel current profile of Fig. 3 at z=0 from the local expression and the profiles of Fig 4. from the integral. They are far from agreement and the local form shows current flowing in the vacuum. The axial variation of the local and integral currents are shown in fig. 5 for a field line in the plasma and one in the vacuum. The differences supply most of the source for eqn. (34). The initial flow patterns in the mid-plane, which is all octupole and higher, and the end plane are in Figs 6,7. The average beta in a plane has a maximum of 8.3%, peak central beta being 25% with $\omega=(1-\Psi/\Psi_{plas})^2$. This case converged in ten steps to 1% accuracy everywhere. Current balance is shown in fig 8 and the convergence behaviour in Figs. 9-12. Note the total current constraint is O(β) smaller than the other measures. Flux surface shapes in equilibrium show the characteristic diamond distortion for a stable equilibrium.

These results agree closely with the dynamical code and quite well with Tebasco, the low-beta analytic equilibrium calculation. The principal differences are that the parallel current is about 15% higher in the finite-β calculation and the geodesic curvatures are somewhat larger. The principal curvature, and hence the MHD stability are hardly altered by the plasma.

At higher betas the code may fail to converge because the initial guess is simply too far from the answer. Also, in tandems with more cells , numerical accuracy becomes a problem. Work is continuing on extending the domain of applicability of the code.

ACKNOWLEDGEMENTS

I would like to thank L.S. Hall, T.B.Kaiser, L.D.Pearlstein for many useful conversations.This work was performed under the auspices of the U.S. Department of Energy by Lawrence Livermore National Laboratory under contract No. W-7405-Eng-48.

REFERENCES.

1. F.Bauer,O.Betancourt, P.Garabedian, A Computational Method for Plasma Equilibrium. Springer, 1978

2. R. Chodura, A. Schluter, J. Comp. Phys,41,68-88,(1981)

3. S. Hirshman, Phys. Fluids, 1983

4. H.R. Strauss, Nucl. Fusion, 22(1982) 893

5. L.D.Pearlstein, B.McNamara, T.B.Kaiser, Bull. A.P.S., Nov. 1983

6. L.D.Pearlstein, T.B.Kaiser, W.A.Newcomb, Phys Fluids, 24(1981)1326

7. J.Johnson, J. Greene, Phys Fluids, 1961

8. R.H.Bulmer et al., Proc. IAEA Conf. on Fusion, 1982 9. L.S.Hall, B. McNamara,Phys. Fluids 18(1975) 552

10. W.A.Newcomb, J. Plasma Phys., 26(1981) Pt3,529

11. T. Kawabe, Private Communication.

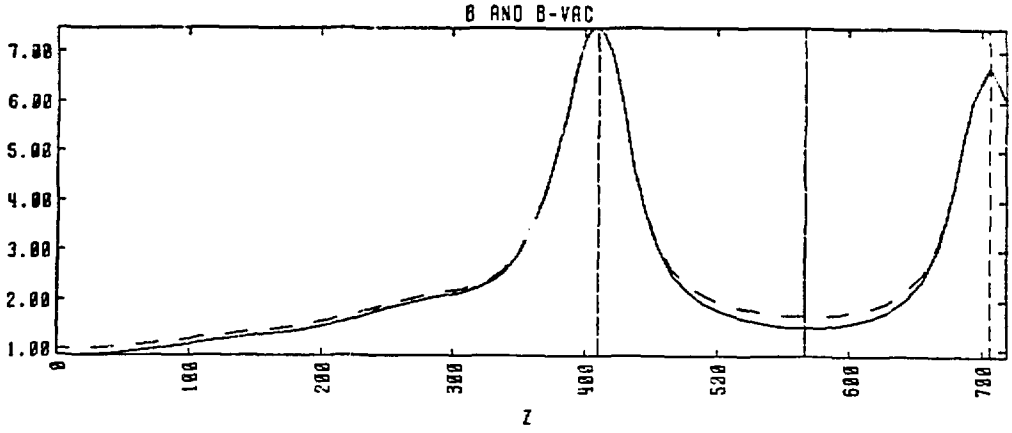

Figs. 1,2. Axial magnetic field strength vs z and the stretched coordinate s(z) to improve accuracy.

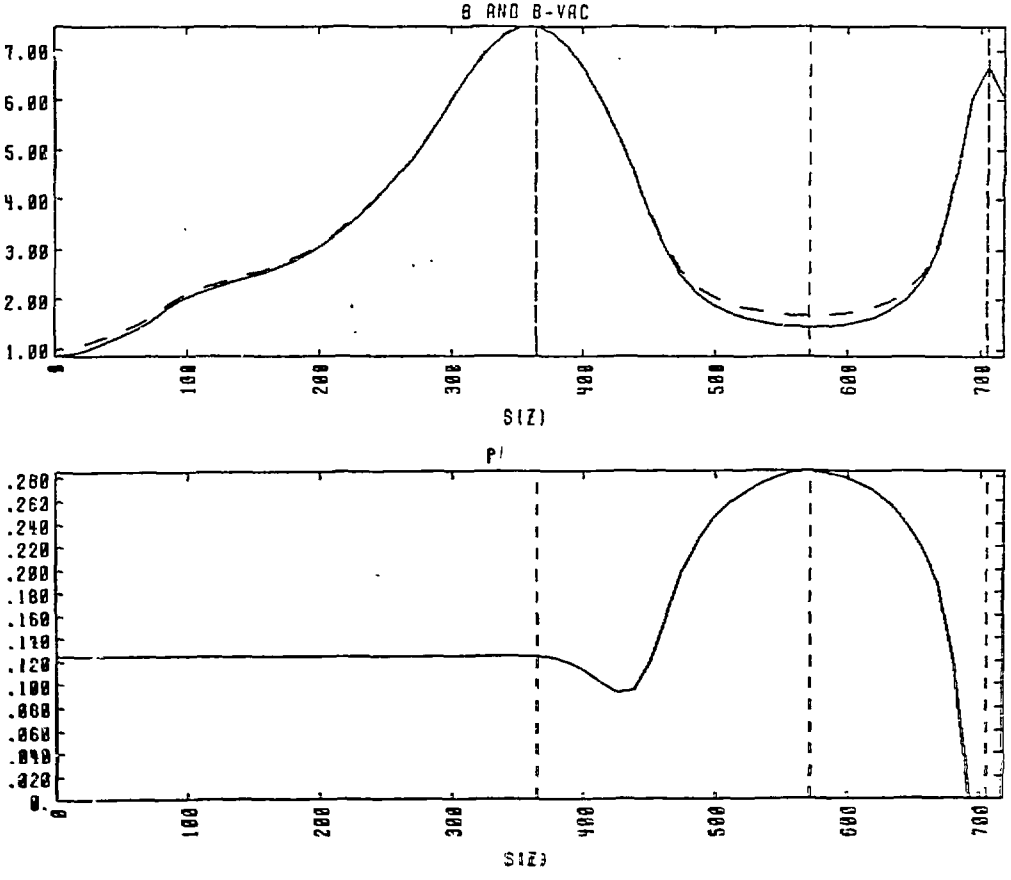

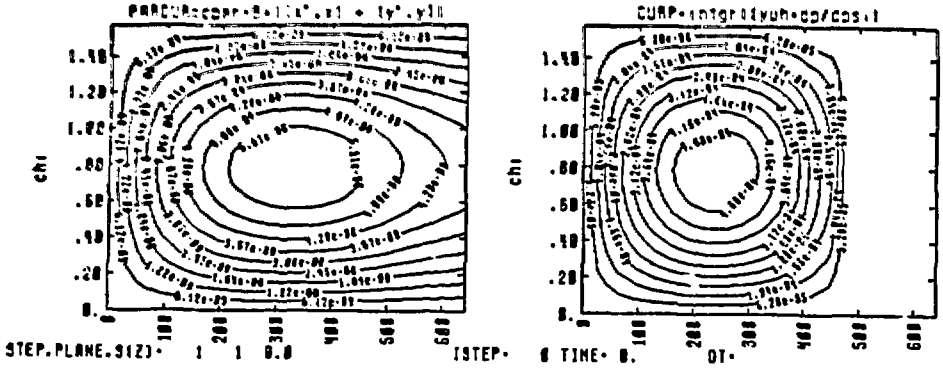

Figs. 3,4. Compare local and integral values of the mid-plane parallel current from the initial guess.

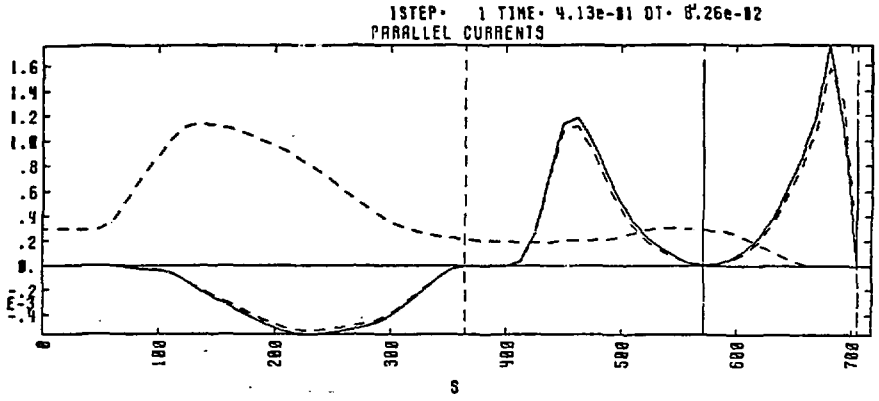

Figs. 5. Solid line is parallel current at $\psi = \psi_{plas}/2$, $\theta = \pi/10$. Nearby dotted line at ψ near ψ wall. Other dotted line is integral value of current on $(\psi_{plas}/2, \pi/10)$.

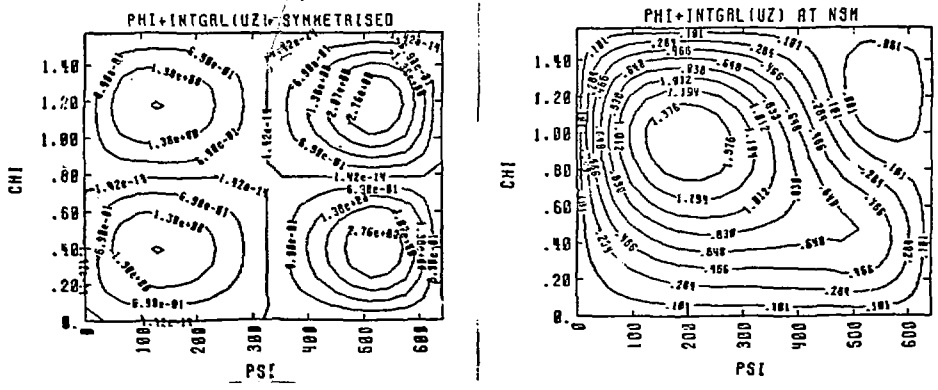

Figs. 6,7. Initial flow pattern in mid-plane and end-plane to approach current balance.

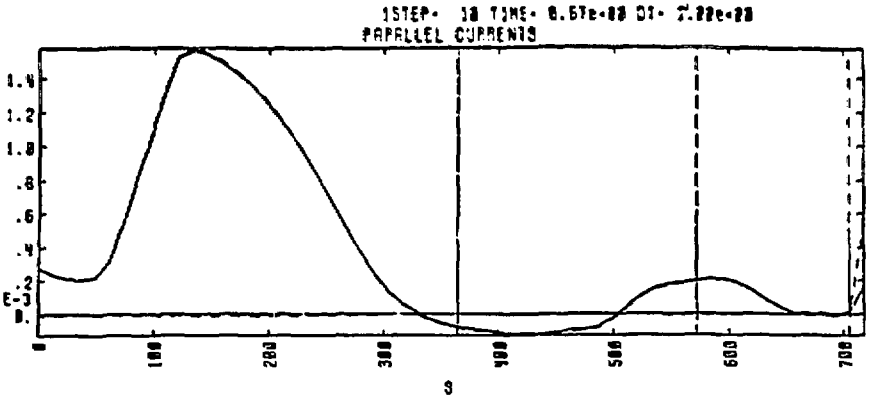

Fig. 8. Local and integral currents balanced in 10 steps. Vacuum currents reduced to zero.

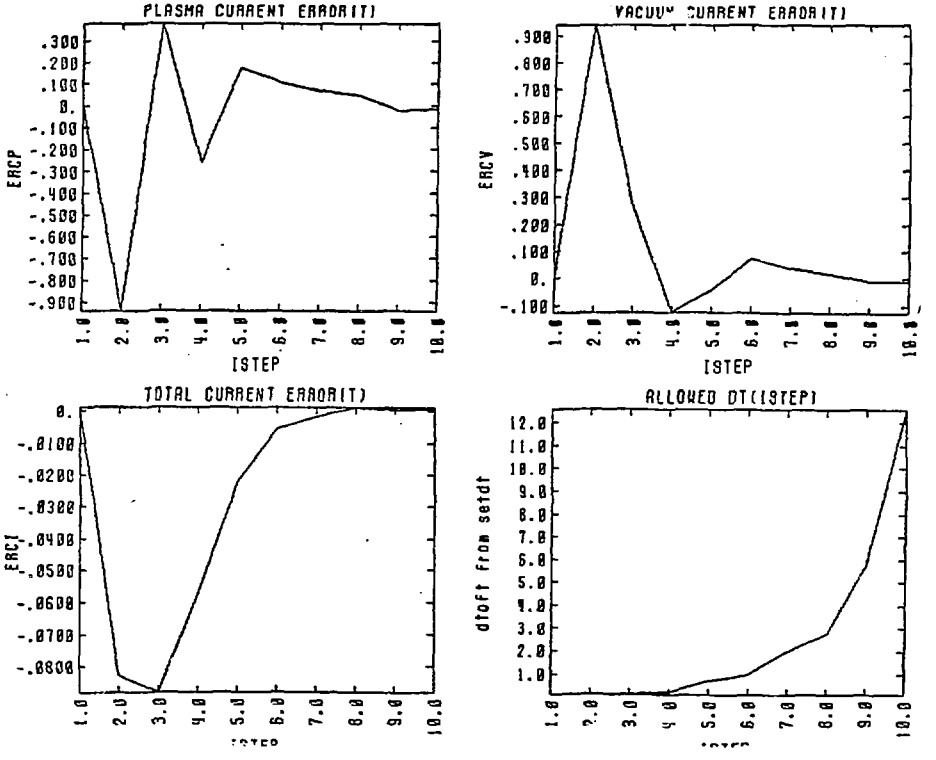

Figs. 9-12. Convergence of relative errors in current balance, vacuum current, ano total current constraint. Also maximum timestep allowed for conserving Jacobian.

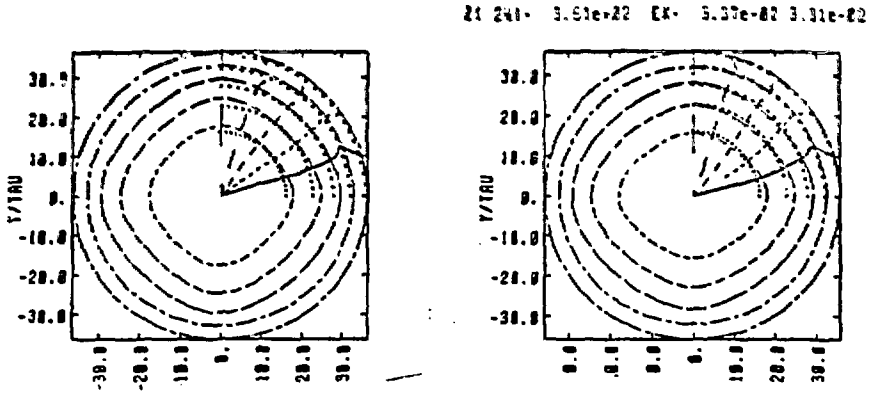

Figs. 13,14. Flux surface shapes in mid-plane and first mirror throat. Coordinates normalized so dotted vacuum shapes are circular.

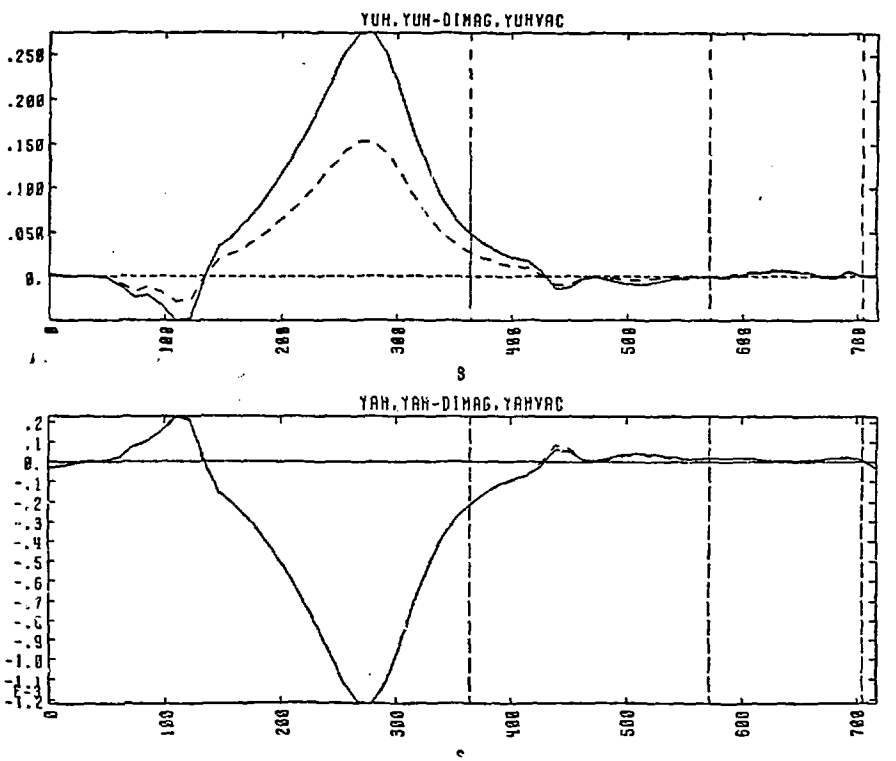

Figs. 15,16. Geodesic and principal curvatures compared with dotted vacuum values.

"Work performed under the auspices of the U.S. Department of Energy by the Lawrence Livermore Laboratory under W-7405-ENG-48."